ORIGINAL ARTICLE

Analytical cut geometry calculation for multi-pass rough milling of a free-form surface machining

H. Hendriko[1], G. Kiswanto[2], A. Akhyan[3], J. Y. Zaira[3], I. Idris[4]

[1] Mechatronics Engineering Department, Politeknik Caltex Riau, Rumbai, Pekanbaru, 28265 Indonesia
 Phone: +6276153939

[2] Laboratory of Manufacturing Technology and Automation, Department of Mechanical Engineering, Universitas Indonesia, Indonesia

[3] Mechanical Engineering Department, Politeknik Caltex Riau, Rumbai, Pekanbaru, 28265 Indonesia

[4] Industrial Engineering Department, Politeknik LP3I Medan, Indonesia

ABSTRACT – This paper presents a simple analytical approach to define cut geometry of multi-pass rough milling during a free-form surface milling. The shape of in-process workpiece surface was identified using the coordinate of corner points that are found in every step of stair-surface. In every instantaneous tool location, the workpiece sections that have possibility intersecting with the cutting edge were identified based on the coordinate of cutter location point. The algorithm was developed for machining using indexable flat end-mill by considering the effect of helix angle to the cut geometry. The proposed method was successfully used to determine the length of cut and generate the shape of cuts. The implementation test also demonstrated that helix angle tends to produce larger cut.The validation of the accuracy was carried out by comparing the length of cut measured using CAD software with those generated by the proposed approach. The results showed that the differences were very small or less than 0.4%. Therefore, it can be taken into conclusion that the method was accurate. The comparison test on computational time was conducted. ABS took only 1.63 second for calculating cut geometry during one tool pass, while Z-mapping method spent 23.21 second. This result proved that ABS is computationally more efficient.

INTRODUCTION

During sculptured surface milling, the machining was normally begined by performing roughing process using 2.5D milling operation. Rough milling is the first stage of material removal process, which is expected to cut the stock material as quickly as possible, and then leaving as thin as possible material allowance for the next process. The dimensional accuracy and machined surface quality are not a concern during material removing process in this stage. Several studies revealed that rough machining process takes more or less 50% of machining time of complex parts manufacturing [1]. Therefore, increasing efficiency during rough machining is very important because it influences significantly the efficiency of overall machining cost. Flat-end cutter is widely used for rough milling because it has longer tool life and higher material removal rate.

Generally, the shape of workpiece material for machining process begins with a block material. Calculating the cut geometry when a vertically straight cutting edge remove a block material is an easy task. In this case, the depth of cut in one tool pass was normally set constant, hence, the length of cutter workpiece intersection is similar to the depth of cut. However, when a rough milling performs multi-pass cutting process during sculpture surface machining, then the surface of the in-process stock material become a complex surface with stair-case profile, as a sample shown in Figure 1a. In this case, the cut geometry calculation become more difficult because the length of cut could be very fluctuated.

Mostly the operator selects the milling parameters from the recommendation of handbooks or based on experience. Normally the parameters were set constant for the whole machining process. In sculptured surface machining, constant parameters tend to produce lower productivity. Various optimization strategies and algorithms have been proposed. In multi-pass rough milling process, the optimization can be performed by reducing the number of passes and optimizing parameters. There are several methodologies that have been proposed to optimize the parameters and distribute the total stock removal into number of tool passes [2]–[4]. Mellal and Williams [2] minimized the total production time by using an algorithm called cuckoo optimization algorithm. Khalilpourazari and Khalilpourazary [4] used robust grey wolf optimizer to improve the parameters used in multi-pass milling. Other researchers enhanced the efficiency of the milling process by optimizing the feedrate profile, or also called feedrate scheduling method [5]–[7].

All the machining optimization methods, which have been proposed, need accurate information about cutter workpiece engagement. There are three major approaches for calculating the cut geometry in a complex milling process, they are solid model, discrete method and analytical method. Solid model can be categorized into constructive solid geometry (CSG) and boundary representation (B-Rep). Spence et al. [8], [9] calculated the cut geometry using CSG to define the cutting force for feedrate scheduling. Lazoglu et al. [10], [11] proposed boundary representation-based method

to define cut geometry of sculptured surface machining in five-axis milling. Although solid model proved that it could be used to determine the cut geometry accurately, but in practical application, it is inefficient due to high computation cost.

Another method that received high attention is discrete method. Discrete method can be classified into vector-based method [12, 13] and polyhedral-based method [14, 15]. Zhang [12] develop cut geometry to support cutting force calculation for free-form surface milling using vector-based method. Meanwhile Aras et al. [14] develop polyhedral method to model removal material during 3-axis milling. Discrete method is recognized efficient in term of computationally time than solid model. However, the computational cost rise significantly as the accuracy is enhanced.

To resolve the problem of high computational cost on solid model and discrete method, several researchers proposed analytical method [16–23]. Gupta et al. [17] developed an analytical approach to define cut geometry in the case of linear half-space and circular cutting. Meanwhile Hendriko et al. [16, 18, 19, 21] developed an analytical method called analytical boundary simulation (ABS) to calculate the engagement between cutting edge and workpiece material in five-axis milling. From a series of tests, the ABS proved that it is accurate and computationally more efficient. However, the algorithm of ABS is applicable for semi-finish and finish milling, but not applicable for rough milling. Improving the efficiency in the stage of rough milling is important because it gives significant effect to overall machining process.

Therefore, this study attempted to expand the ABS method so that it could be used to define the cut geometry of multi-pass rough milling for complex surface machining. The algorithm was developed for machining using indexable flat end-mill. Flat-end mill is widely used for rough milling due to the higher material removal rate. The shape of in-process workpiece surface was indicated using the coordinate of corner points that are found on the corner of the stair surface, as illustrated in Figure 1(b). Moreover, the algorithm developed in this study took into consideration the effect of helix angle on the cutting edge.

OBTAINING CUTTER WORKPIECE ENGAGEMENT POINTS

The length of cut is defined as length of cutting edge intersect with the workpiece, which is measured from the uppermost intersection point (UI-point) to the lowermost intersection point (LI-point). The UI-point and the LI-point are the end points of cutter workpiece engagement. The UI-point is denoted by $n_f\left(x_{n_f}, y_{n_f}, z_{n_f}\right)$, while the LI-point is represented by $C_f(x_{C_f}, y_{C_f}, z_{C_f})$. The length of cut could be calculated after these two points are obtained.
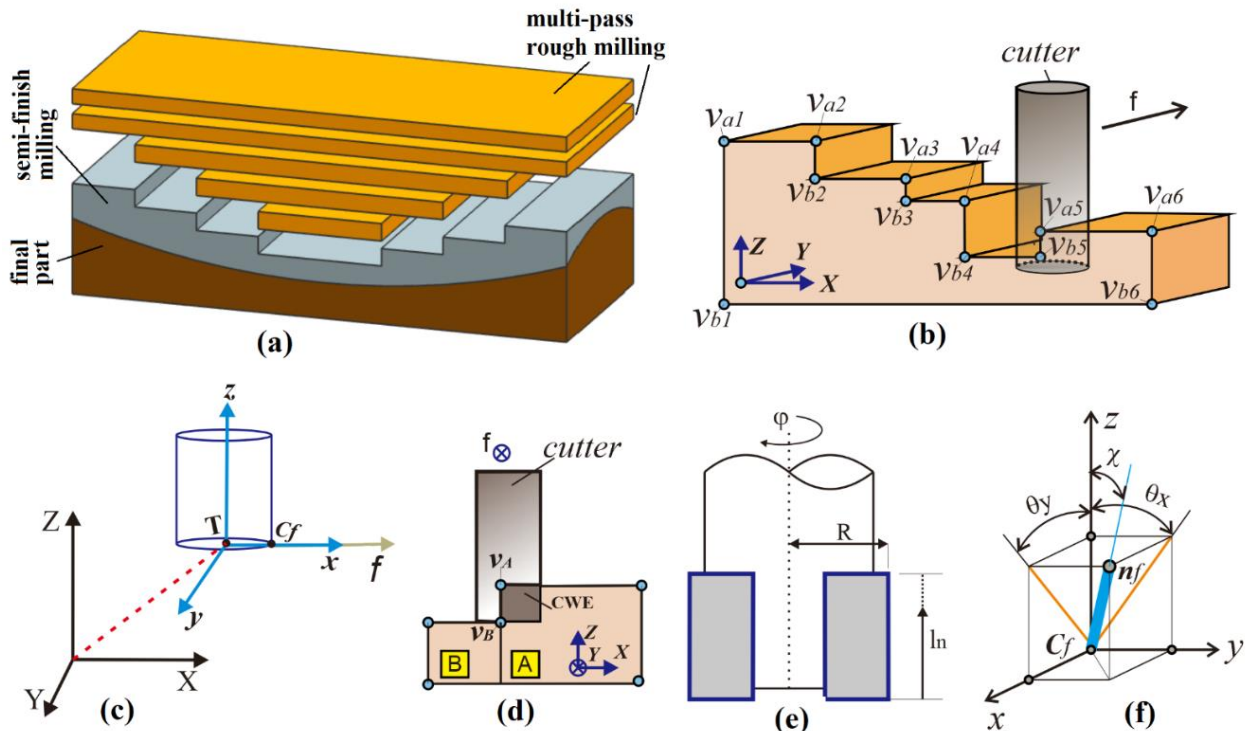

Figure 1. (a) multi-pass rough milling, (b) workpiece representation method for rough milling, (c) coordinate systems, (d) CWE region and workpiece sections, (e) flat-end tool and (f) cutting edge orientation due to helix angle

To define the position of cutter, the coordinate systems were established as shown in Figure 1(c). They are workpiece coordinate system (WCS) and tool coordinate system (TCS). WCS is denoted by the vector X, Y, Z and was used as the reference coordinate system. Meanwhile, TCS was set at the bottom center of cutter and indicated by x, y, z. In every cutter position, $T(x_T, y_{T,} z_T)$, the border wall of workpiece material that has potential engage with cutter should be

identified. By assuming that cutter moves in Y-axis, then the potential engaging walls are located in between the coordinate of $\left((x_T + R), y_T, z_T\right)$ and $\left((x_T - R), y_T, z_T\right)$, where R is the radius of cutter. For the condition as shown in Figure 1(d), there are two points that were detected based on the position of cutter, they are denoted as $v_A(x_{v_A}, y_{v_A}, z_{v_A})$ and $v_B(x_{v_B}, y_{v_B}, z_{v_B})$. It means that there is only one wall that has potential engage with cutter. The wall was constructed by two workpiece sections that are called section A and section B. Section A is a workpiece section that engages with the cutter contact point $C(x_C, y_C, z_C)$, while section B is a workpiece section next to the section A that has potential intersects with cutter.

The shape of flat-end mill, as shown in Figure 1(e), was considered as a cylinder and it was calculated parametrically using the equation below:

$$S_C(\varphi; l) = \begin{bmatrix} R \sin \varphi \\ R \cos \varphi \\ l_n \end{bmatrix} \quad ; 0 < l_n < l \tag{1}$$

where φ is the cutter rotation angle and l_n is distance of point on the surface that was measured from the bottom of cutter. l_n was also used to define the length of cut, which is the distance between UI-point (n_f) and LI-point (C_f), as illustrated in Figure 2(a) and Figure 2(b).

The coordinate of LI-point with regards to the tool rotation angle was expressed by:

$$C_f\left(x_{C_f}, y_{C_f}, z_{C_f}\right) = S_C(\varphi; l_n = 0) + T \tag{2}$$

When rough milling process using cutter without helix angle, then the cutting tool performs plain cutting. It means that the length of cut is similar to the axial depth of cut. The cutting edge intersects with only one workpiece section and the UI-point coincides with the top surface of workpiece section. The coordinate of UI-point was determined as follow

$$n_f\left(x_{n_f}, y_{n_f}, z_{n_f}\right) = S_C\left(\varphi; l_n = z_{v_A} - z_T\right) + T; \rightarrow \text{if } x_{C_f} < x_{v_A} \text{ and } z_{C_f} < z_{v_A} \tag{3}$$

$$n_f\left(x_{n_f}, y_{n_f}, z_{n_f}\right) = S_C\left(\varphi; l_n = z_{v_B} - z_T\right) + T; \rightarrow \text{if } x_{C_f} > x_{v_A} \text{ and } z_{C_f} < z_{v_B} \tag{4}$$

Then the length of cut was calculated as follow:

$$L = z_{n_f} - z_{C_f} \tag{5}$$

CUT GEOMETRY CALCULATION FOR TOOL WITH HELIX ANGLE

Determining cut geometry of a flat-end cutter with helix angle during roughing process is more complex than the tool without helix angle. The helix angle inclines the orientation of cutting edge and makes the orientation of cutter is continuously changed for every tool rotation angle, hence, the calculation become more complex. The effect of helix angle to the orientation of cutter has been discussed by Hendriko [18], [23].

The existence of helix angle do not influences the coordinate of LI-point, but the coordinate of UI-point. Therefore, Eq. (2) could be used to calculate the LI-point of helix cutting edge. The equation to determine the UI-point of helix cutting-edge yields to:

$$n_f\left(x_{n_f}, y_{n_f}, z_{n_f}\right) = [M]_h . S_C\left(\varphi; l_n = z_{v_A} - z_T\right) + T; \rightarrow \text{if } x_{C_f} < x_{v_A} \text{ and } z_{C_f} < z_{v_A} \tag{6}$$

$$n_f\left(x_{n_f}, y_{n_f}, z_{n_f}\right) = [M]_h . S_C\left(\varphi; l_n = z_{v_B} - z_T\right) + T; \rightarrow \text{if } x_{C_f} > x_{v_A} \text{ and } z_{C_f} < z_{v_B} \tag{7}$$

where $[M]_h$ is a transformation operator when helix angle exists, which involved the cutting-edge orientation angle about X-axis (θ_X) and Y-axis (θ_Y). The orientation angles of the cutting edge with regards to TCS is presented in Figure 1(f). The method to obtain the cutting-edge orientation angles, θ_X and θ_Y was explained in [16, 18]. The transformation operator is determined as follow,

$$[M]_h = Rot(X, \theta_X) . Rot(Y, \theta_Y)$$

$$[M]_h = \begin{bmatrix} \cos \theta_Y & 0 & \sin \theta_Y \\ \sin \theta_X \sin \theta_Y & \cos \theta_X & -\sin \theta_X \cos \theta_Y \\ -\cos \theta_X \sin \theta_Y & \sin \theta_X & \cos \theta_X \cos \theta_Y \end{bmatrix} \tag{8}$$

The helix angle modifies the orientation of cutter. Due to the inclination angle, the cutting edge does not only intersect with one workpiece section, but it could also intersect with two or more workpiece sections. In addition, the UI-point is not only located on the top surface, but it could be also located on the wall surface. When the direction of cutting edge is not vertically straight with respect to WCS, then the UI-point was determined using an approach called the *Cylindrical-Surface method*. In this case, the length between the LI-point to the surface of workpiece section is required to calculate the UI-point. By assuming that the feed direction is along the Y-axis, then the Cylindrical-boundary method consists of two methods based on the location of the UI-point, they are *Z-Cylindrical method* and *X-Cylindrical method*.
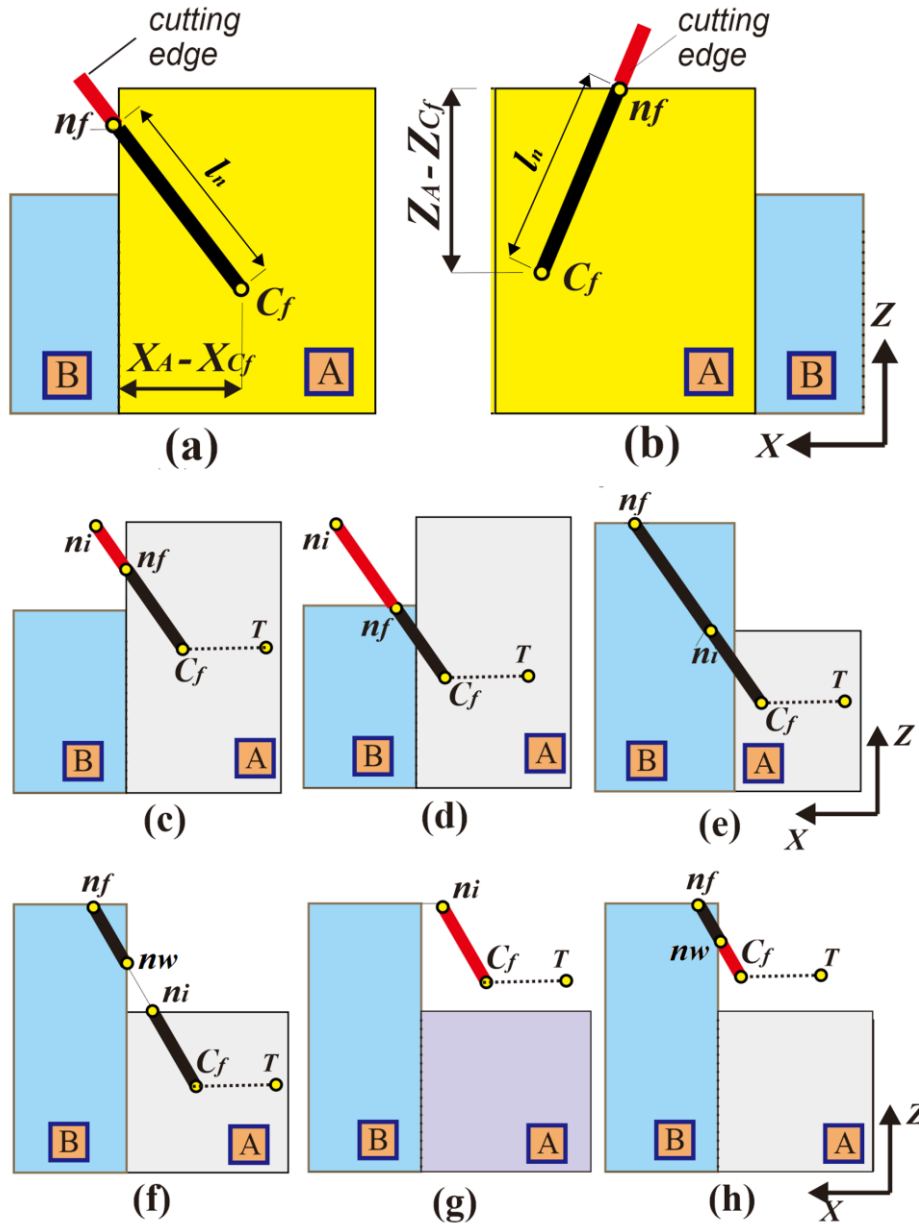

Figure 2. Various possible location of the UI-point on the workpiece sections during tool rotation

X-Cylindrical method: this method was applied when the UI-point was coincided with the wall surface. The length between the LI-point to the wall surface in the X-axis (l_n), as shown in Figure 2(a), can be determined as follows,

$$l_n = \left(x_A - x_{C_f}\right) / \tan \theta_X \, \cos \chi = \left(x_A - x_{C_f}\right) / \sin \theta_Y \tag{9}$$

Z-Cylindrical method: this method was applied when the UI-point was coincided with the top surface of workpiece section. In this case, the length between the LI-point to the top surface of the workpiece section on the Z-axis (l_n), as shown in Figure 2(b), was calculated as follows,

$$l_n = \left(z_A - z_{C_f} \right) / \cos \chi \tag{10}$$

where, z_{C_f} and z_A are the Z-axis of the LI-point and the Z-axis of the top surface of workpiece section, consecutively.
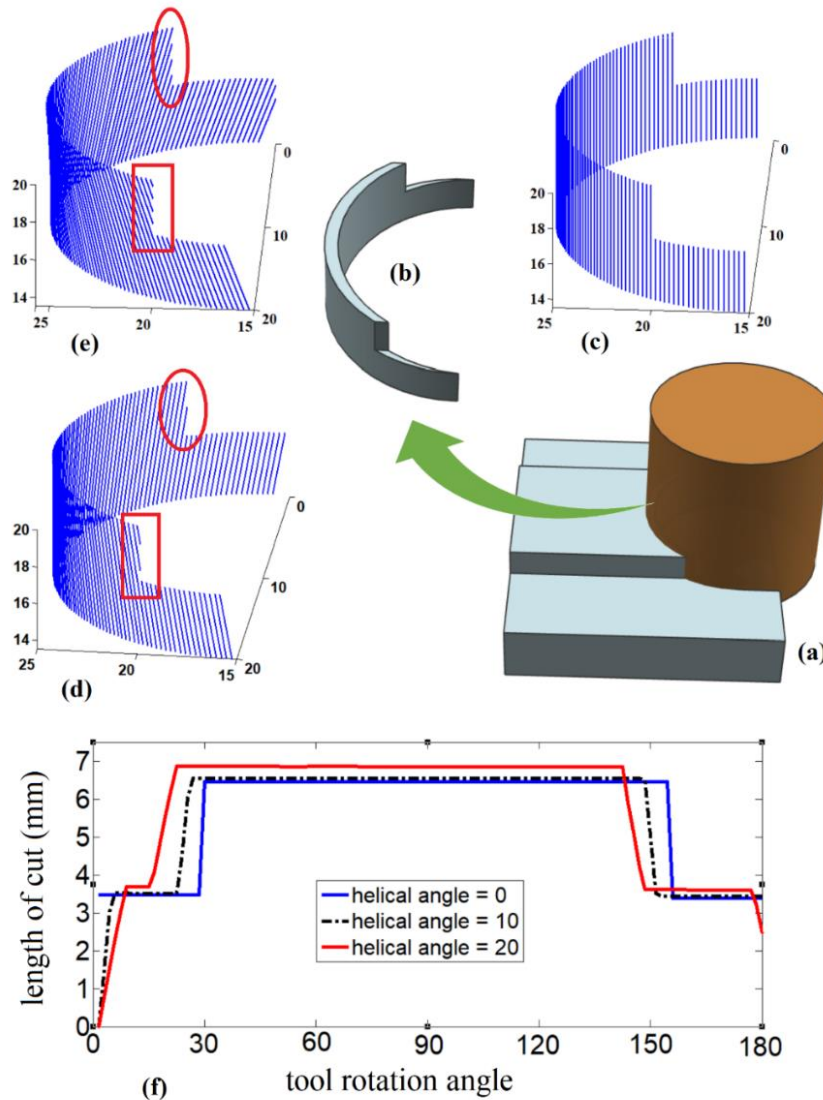

Figure 3. Test model: (a) part model, (b) cutter geometry model, (c) cut geometry of cutter without helix angle, (d) cut geometry of cutter with helix angle 10, (e) cut geometry of cutter with helix angle 20 and (f) the length of cuts

Initially, the calculation was presumed that the UI-point is coincided with the top surface of workpiece section A. Then, Z-Cylindrical method was applied to determine the tentative UI-point $n_i(x_{n_i}, y_{n_i}, z_{n_i})$. It was called the tentative UI-point because it should be verified to confirm whether or not it was on the top surface of section A. The tentative UI-point was considered wrong if $x_{n_i} < x_A$, then the actual UI-point, $n_f\left(x_{n_f}, y_{n_f}, z_{n_f}\right)$, need to be determined. In this case, some inspection should be carried out to find the actual UI-point. The whole steps to obtain the actual UI-point are explained below,

1. When $z_A > z_B$ and $x_{n_i} > x_B$ and $z_{n_i} > z_B$, then the UI-point coincides either with the wall of section A, as illustrated in Figure 2(c), or with the top surface of section B, as depicted in Figure 2(d). Both of possibilities should be inspected to define the actual UI-point.

2. When $z_A < z_B$ and $x_{n_i} > x_B$ and $z_{C_f} < z_A$, then the UI-point coincides with the top surface of workpiece section B as illustrated in Figure 2(e).

3. When $z_A < z_B$ and $x_{n_i} < x_B$ and $z_{C_f} < z_A$, then the actual UI-point could be calculated after the intersection point on the wall surface, $n_w(x_w, y_w, z_w)$, was obtained. If $z_w < z_B$, then the actual UI-point coincides with the top

surface of section B as denoted in Figure 2(f). In this case, the cutting edge intersects with two workpiece sections, but some part of cutting edge within two intersection points is separated with workpiece section. Otherwise, the UI-point coincides with the top surface of section A.

4. When $z_A < z_B$ and $z_{C_f} > z_A$ and $z_w > z_B$: in this case, there is no engagement between cutting edge and workpiece section as shown in Figure 2(g).

5. When $z_A < z_B$ and $z_{C_f} > z_A$ and $z_w < z_B$: then the UI-point coincide with the wall surface of section B as illustrated in Figure 2(h).

When the UI-point coincides with the top surface of workpiece section, then the *Z-Cylindrical* method was applied to determine the intersection point. On the other hand, when the UI-point coincides with the wall surface of workpiece section, then the UI-points point are calculated using the *X-Cylindrical* method.

In the case of workpiece material is a high staircase (the workpiece sections are small) was machined using a large cutter, then there is a possibility that the cutting edge intersects with more than two workpiece sections. In that instance, the UI-point can be coincided with the section surface next to the section B. Then the calculation was performed by continuously checking and calculating the intersection point until the actual intersection point is obtained.

RESULT AND DISCUSSION

All the algorithm presented in previous section have been implemented to build a cut geometry calculation program using MATLAB. In this study, the implementation test and verification test were performed using simulation program. The proposed approach was examined using two model cases. In the first test, a rough machining process as shown in Figure 3(a) was performed using a two-teeth flat-end cutter with 20 mm diameter. Cutting parameters employed in the implementation test were spindle speed 5000 rpm and feedrate 0.3 mm/tooth. The test was also aimed to examine the influence of helix angle to the length of cut. Therefore, two types of cutter were used to ensure the applicability of the proposed method, they were the cutter with and without helix angle. For the first test, three helix angles were used, they are 0, 10, and 20.
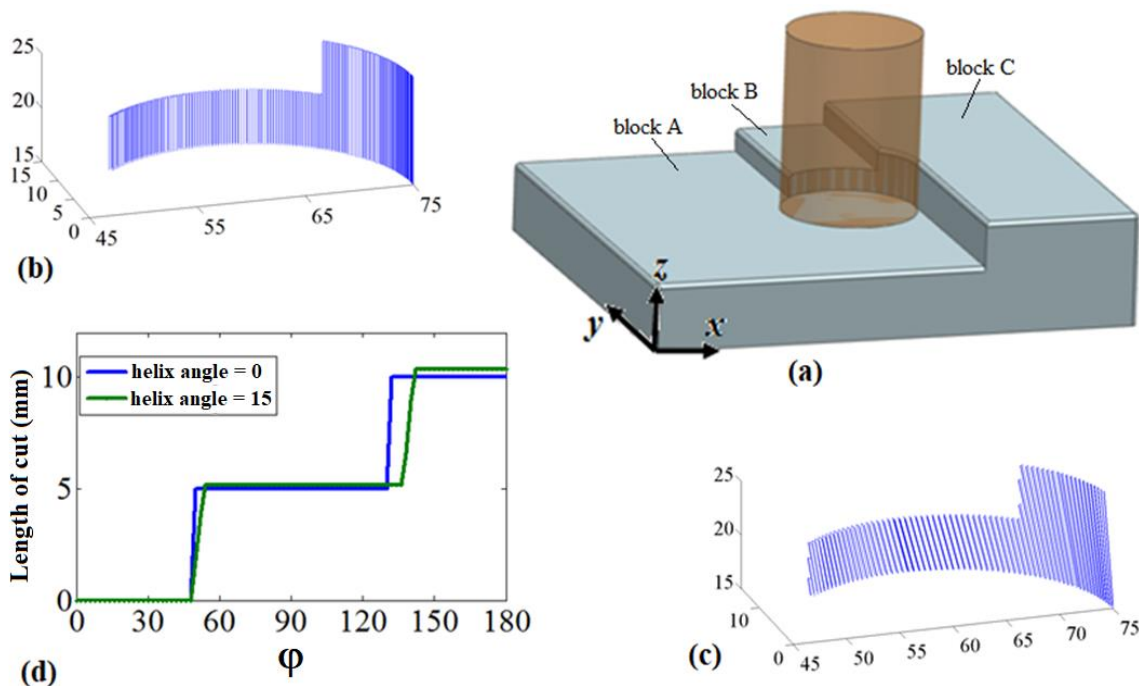

Figure 4. Test model: (a) part model, (b) cut geometry of cutter without helix angle, (c) cut geometry of cutter with helix angle and (d) the length of cuts

The test model as shown in Figure 3(a) was developed using Siemens-NX. The shape of intersection between cutter and workpiece for one tool rotation was extracted and presented in Figure 3(b). The instantaneous cut geometry can be obtained using the developed program as samples shown in in Figure 3(c) - Figure 3(e). Figure 3(c) depicted the geometry of cut when cutter without helix angle. The geometry of cuts when the helix angle exist were shown in Figure 3(c) (helix angle 10) and Figure 3(e) (helix angle 20). The shape of cut generated using simulation program, which were presented in Figure 3(c) - Figure 3(e), similar to the shape of intersection model generated using Siemens-NX as shown in Figure

3(b). It is an indication that the algorithm developed was accurate. In the case of the tool without helix angle, all the UI-points coincided with the top surface of the section. However, when the inclination angle exists, then the UI-point could be either on the top surface of the workpiece section or on the wall surface of the workpiece section. The cuts, which are highlighted using ellipse in Figure 3(d) and Figure 3(e), display the conditions when the UI-point coincided with the wall surface of workpiece section. Meanwhile, the cuts, which are highlighted using rectangular in Figure 3(d) and Figure 3(e), show the case of cutting edge in between two intersection points were out of sections as illustrated in Figure 2(f).

The length of cut for all the test were presented in Figure 3(f). The graphs showed that the cutting edge with helix angle tend to produce longer cut when the engagement occurred on the top surface. Larger helix angle generates longer cut. The longest cut produced by cutting edge without helix angle is 6.45 mm. Meanwhile cutting edge with helix angle 10° and 20° produced 6.55 mm and 6.86 mm the longest cut, consecutively. The tool without helix angle engaged the workpiece material completely since beginning. On the other hand, the cutting edge entered the workpiece gradually when the tool with helix angle. Cutting edge with helix angle 10° engaged completely with the first wall at tool rotation angle (φ) 10°. Meanwhile cutting edge with helix angle 20° engaged completely with the same wall at tool rotation angle 15°. The gradual engagement between cutter and workpiece is one of the main purposes of helix angle.

The second test was performed for the case of milling process as shown in Figure 4(a). In this test, two cutters with 30 mm diameter were employed. They are the cutter without helix angle and the cutter with helix angle 15°. The shape of cuts for one tool rotation were generated using simulation program and the results presented in Figure 4(b) and Figure 4(c). In this case, the tool passed three workpiece sections (section A, section B, and section C), however, only two workpiece sections (section B, and section C) engaged with the cutting edge. The tool passed over the section A, and hence, there is no engagement between cutting edge and the workpiece section A. It can be seen in Figure 4(d) that there was no cutter workpiece intersection in beginning. The engagement between cutter and section A at tool rotation 50°. This was the case as illustration in Figure 2(g). Once again, the test demonstrated that cutter with helix angle prone to produce longer cuts. In this test, the longest cut produced by cutter with helix angle 15° is 10.35 mm. Meanwhile, cutter without helix angle produced 10 mm the longest cut.
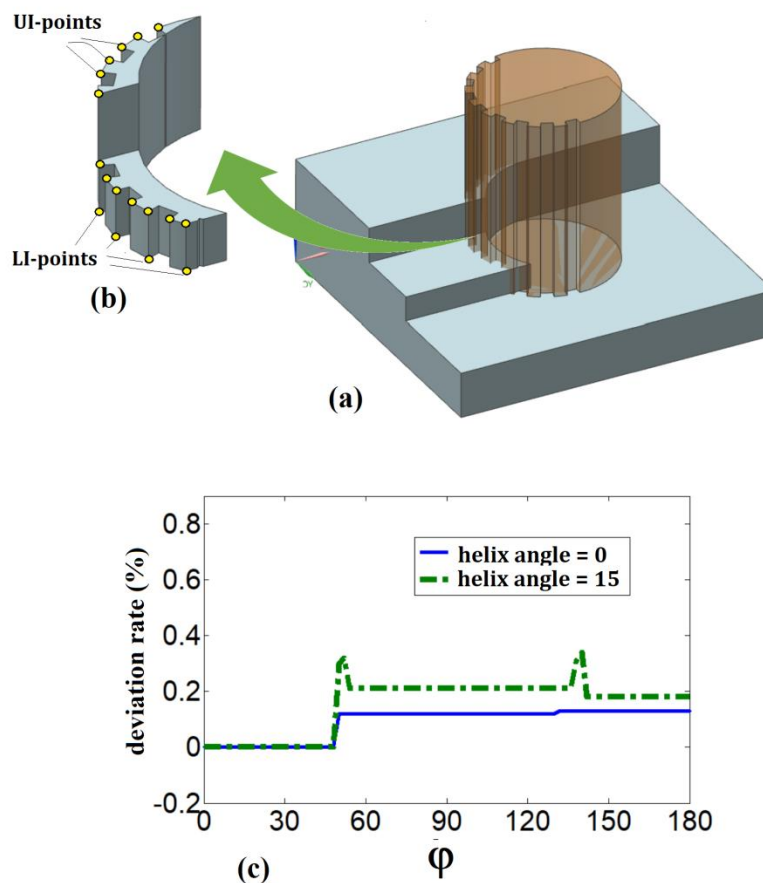

Figure 5. (a) Test model, (b) extraction model and (c) deviation rate

Although the geometry of cut obtained using the simulation program similar to the cut model extracted using Siemens-NX, the accuracy of the proposed approach needed to be validated. The accuracy was checked by measuring the length of cuts using Siemens-NX, and then comparing with those calculated using simulation program. For the validation purpose, the model of cutter was modified as shown in Figure 5(a). The grooving at the front side was aimed to identify easily the rotation angle of cut geometry. Once the cut geometry was extracted, as presented in Figure 5(b), the length of

cut for every groove can be measured. The validation was performed for every 2 degree of tool rotation angle and the results were presented in Figure 5(c). There is no error in beginning because there is no engagement between cutter and workpiece. The errors when the enggagement occurred on the wall surface are slightly higher than the engagement on the the top surace. In this test, all the length of cuts determined using the developed method and those obtained using Siemens-NX have very small differences (less than 0.4%). Therefore, it can be taken into conclusion that the method was accurate.

The main advantage of analytical methods compare to numerical and discrete methode is efficient computational time. Therefore, computational test needs to be performed to ensure the efficiency of the proposed method. In this study, the computational time of ABS method was compared to the Z-mapping method. Z-mapping is a discrete based method that is widely used for calculating cut geometry. The comparison test was performed using the workpiece surface and cutting tool model as shown in Figure 4(a). For Z-mapping method, the workpiece surface was discritized with a grid size 0.15 mm. Meanwhile for ABS, there was no necessary to define grid size because there was no correlation between grid size and computational time. The intensity of cut geometry data generated by ABS method was set at every 2° of tool rotation.

The test was perfomed using Matlab on laptop with processor Intel(R) Core i7-7500 CPU 2.7 GHz and 16 GB RAM. An uninterupped test for one tool pass which contain 41 CC-points was executed. The test on every method was repeated three time and the average results are provided in Figure 6. ABS method took only 1.63 second to calculate the cut geometry for one tool pass. Meanwhile Z-mapping method spent 23.21 second. The graph in Figure 6 presents clearly the efficiency of ABS method over Z-mapping method. The Z-mapping produced long computational time because it has to scan and calculate a huge amount of discrete vector.
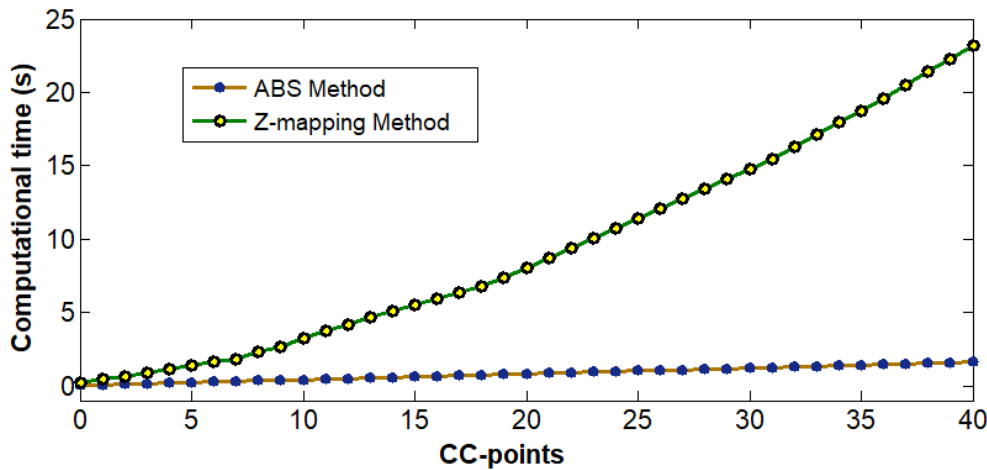

Figure 6. Comparison test on computational time between ABS and Z-mapping

CONCLUSION

In this study, the method called the analytical boundary simulation (ABS) was successfully extended for calculating the cut geometry of multi-stage roughing milling. The developed method considered the effect of helix angle to the length of cut. The uppermost intersection point was calculated using *Cylindrical-Surface* method, which was consist of *Z-Cylindrical* method and *X-Cylindrical* method. Several tests were performed to check the applicability of the proposed method. The primary contributions of this study include as follow:

1. The proposed method has been tested to check the implementability in calculating the geometry of cut. The test was performed using simulation software, Matlab. The implementation tests demonstrated that the proposed approach can be used to determine the cut geometry during rough milling process. The developed program could provide the information on the size of cut and generate the shape of cut.

2. The tests were also performed for checking the effect of helix angle to the length of cut. The results showed that the existence of helix angle tends to generate longer cut. Increasing helix angle will increase the length of cut.

3. The validation test to check the accuracy of the proposed method was conducted by measuring the length of cuts using Siemens-NX, and then comparing with those calculated using simulation program. The results showed that the diffrence were very small (less than 0.4%). It confirmed that the developed method was accurate.

4. Comparison test on computational time between ABS and Z-mapping method was performed. The result showed that ABS took only 1.63 second for calculating cut geometry during one tool pass, while Z-mapping method spent 23.21 second. This result proved that ABS is computationally efficient.

5. In this study, the implementation test and verification to check the accuracy of the proposed method were conducted using simulation softwares, Matlab and Siemens-NX. In the future, the verification will be conducted experimentally.

ACKNOWLEDGEMENTS

REFERENCES

[1]   Z. Yao and S. K. Gupta, "Cutter path generation for 2.5D milling by combining multiple different cutter path patterns," *Int. J. Prod. Res.*, vol. 42, no. 11, pp. 2141–2161, 2004, doi: 10.1080/00207540310001652879.

[2]   M. A. Mellal and E. J. Williams, "Total production time minimization of a multi-pass milling process via cuckoo optimization algorithm," no. mm, 2016, doi: 10.1007/s00170-016-8498-3.

[3]   J. Huang, L. Gao, and X. Li, "An effective teaching-learning-based cuckoo search algorithm for parameter optimization problems in structure designing and machining processes," *Appl. Soft Comput. J.*, vol. 36, pp. 349–356, 2015, doi: 10.1016/j.asoc.2015.07.031.

[4]   S. Khalilpourazari and S. Khalilpourazary, "Optimization of production time in the multi-pass milling process via a Robust Grey Wolf Optimizer," *Neural Comput. Appl.*, vol. 29, no. 12, pp. 1321–1336, 2018, doi: 10.1007/s00521-016-2644-6.

[5]   L. Lu, L. Zhang, S. Ji, Y. Han, and J. Zhao, "An offline predictive feedrate scheduling method for parametric interpolation considering the constraints in trajectory and drive systems," *Int. J. Adv. Manuf. Technol.*, vol. 83, no. 9–12, pp. 2143–2157, 2016, doi: 10.1007/s00170-015-8112-0.

[6]   Y. Liang, J. Ren, D. Zhang, X. Li, and J. Zhou, "Mechanics-based feedrate scheduling for multi-axis plunge milling," *Int. J. Adv. Manuf. Technol.*, vol. 79, no. 1–4, pp. 123–133, 2015, doi: 10.1007/s00170-015-6807-x.

[7]   H. Ni, T. Hu, C. Zhang, S. Ji, and Q. Chen, "An optimized feedrate scheduling method for CNC machining with round-off error compensation," *Int. J. Adv. Manuf. Technol.*, vol. 97, no. 5–8, pp. 2369–2381, 2018, doi: 10.1007/s00170-018-1986-x.

[8]   A. D. Spence, F. Abrari, and M. A. Elbestawi, "Integrated solid modeller based solutions for machining," *CAD Comput. Aided Des.*, vol. 32, no. 8–9, pp. 553–568, 2000, doi: 10.1016/S0010-4485(00)00042-7.

[9]   Y. Altintas and A. D. Spence, "Solid modellers based milling process simulation and planning system," *Am. Soc. Mech. Eng. Prod. Eng. Div. PED*, vol. 56, no. June 1992, pp. 65–79, 1992.

[10]   I. Lazoglu, Y. Boz, and H. Erdim, "Five-axis milling mechanics for complex free form surfaces," *CIRP Ann. - Manuf. Technol.*, vol. 60, no. 1, pp. 117–120, 2011, doi: 10.1016/j.cirp.2011.03.090.

[11]   Y. Boz, H. Erdim, and I. Lazoglu, "A comparison of solid model and three-orthogonal dexelfield methods for cutter-workpiece engagement calculations in three- and five-axis virtual milling," *Int. J. Adv. Manuf. Technol.*, vol. 81, no. 5–8, pp. 811–823, 2015, doi: 10.1007/s00170-015-7251-7.

[12]   L. Zhang, "Process modeling and toolpath optimization for five-axis ball-end milling based on tool motion analysis," *Int. J. Adv. Manuf. Technol.*, vol. 57, no. 9–12, pp. 905–916, 2011, doi: 10.1007/s00170-011-3354-y.

[13]   L. Zhang, J. Feng, Y. Wang, and M. Chen, "Feedrate scheduling strategy for free-form surface machining through an integrated geometric and mechanistic model," *Int. J. Adv. Manuf. Technol.*, vol. 40, no. 11–12, pp. 1191–1201, 2009, doi: 10.1007/s00170-008-1424-6.

[14]   E. Aras and D. Yip-Hoi, "Geometric modeling of cutterlworkpiece engagements in three-Axis milling using polyhedral representations," *J. Comput. Inf. Sci. Eng.*, vol. 8, no. 3, pp. 0310071–03100713, 2008, doi: 10.1115/1.2960490.

[15]   G. S. Bolaños, S. Bedi, and S. Mann, "A topological-free method for three-axis tool path planning for generalized radiused end milled cutting of a triangular mesh surface," *Int. J. Adv. Manuf. Technol.*, vol. 70, no. 9–12, pp. 1813–1825, 2014, doi: 10.1007/s00170-013-5450-7.

[16]   H. Hendriko, N. Khamdi, and J. Jaenudin, "Implementation of an analytical inverse kinematics simulation method for a 5-DOF parallel manipulator," *J. Eng. Sci. Technol.*, vol. 14, no. 4, pp. 1948–1959, 2019.

[17]   S. K. Gupta, S. K. Saini, B. W. Spranklin, and Z. Yao, "Geometric algorithms for computing cutter engagement functions in 2.5D milling operations," *CAD Comput. Aided Des.*, vol. 37, no. 14, pp. 1469–1480, 2005, doi: 10.1016/j.cad.2005.03.001.

[18]   H. Hendriko, G. Kiswanto, J. Istiyanto, and E. Duc, "Implementation of analytical boundary simulation method for cutting force prediction model in five-axis milling," *Mach. Sci. Technol.*, vol. 22, no. 1, pp. 163–179, 2018, doi: 10.1080/10910344.2017.1337130.

[19]   H. Hendriko, "Cut geometry calculation for the semifinish five-axis milling of nonstraight staircase workpieces," *J. Mech. Sci. Technol.*, vol. 34, no. 3, pp. 1301–1311, 2020, doi: 10.1007/s12206-020-0229-x.

[20]   L. T. Tunc and E. Budak, "Extraction of 5-axis milling conditions from CAM data for process simulation," *Int. J. Adv. Manuf. Technol.*, vol. 43, no. 5–6, pp. 538–550, 2009, doi: 10.1007/s00170-008-1735-7.

[21]   H. Hendriko, "Mathematical model for calculating scallop height of toroidal cutter in five-axis milling," *ARPN J. Eng. Appl. Sci.*, vol. 12, no. 19, 2017.

[22]   B. Ozturk and I. Lazoglu, "Machining of free-form surfaces. Part I: Analytical chip load," *Int. J. Mach. Tools Manuf.*, vol. 46, no. 7–8, pp. 728–735, 2006, doi: 10.1016/j.ijmachtools.2005.07.038.

[23]   H. Hendriko, "A hybrid analytical and discrete based methodology to calculate path scallop of helical toroidal cutter in five-axis milling," *FME Trans.*, vol. 46, no. 4, 2018, doi: 10.5937/fmet1804552H.